

Association of the Vaccinia Virus A11 Protein with the Endoplasmic Reticulum and Crescent Precursors of Immature Virions

Liliana Maruri-Avidal, Andrea S. Weisberg, Bernard Moss

Laboratory of Viral Diseases, National Institute of Allergy and Infectious Diseases, Bethesda, Maryland, USA

The apparent *de novo* formation of viral membranes within cytoplasmic factories is a mysterious, poorly understood first step in poxvirus morphogenesis. Genetic studies identified several viral proteins essential for membrane formation and the assembly of immature virus particles. Their repression results in abortive replication with the accumulation of dense masses of viroplasm. In the present study, we further characterized one of these proteins, A11, and investigated its association with cellular and viral membranes under normal and abortive replication conditions. We discovered that A11 colocalized in cytoplasmic factories with the endoplasmic reticulum (ER) and L2, another viral protein required for morphogenesis. Confocal microscopy and subcellular fractionation indicated that A11 was not membrane associated in uninfected cells, whereas L2 still colocalized with the ER. Cell-free transcription and translation experiments indicated that both A11 and L2 are tail-anchored proteins that associate post-translationally with membranes and likely require specific cytoplasmic targeting chaperones. Transmission electron microscopy indicated that A11, like L2, associated with crescent membranes and immature virions during normal infection and with vesicles and tubules near masses of dense viroplasm during abortive infection in the absence of the A17 or A14 protein component of viral membranes. When the synthesis of A11 was repressed, “empty” immature-virion-like structures formed in addition to masses of viroplasm. The immature-virion-like structures were labeled with antibodies to A17 and to the D13 scaffold protein and were closely associated with calnexin-labeled ER. These studies revealed similarities and differences between A11 and L2, both of which may be involved in the recruitment of the ER for virus assembly.

Poxvirus morphogenesis occurs in discrete factories within the cytoplasm of infected cells (1). Although the general features are similar in all members of the family, the process has been most extensively studied with vaccinia virus (VACV). The first distinguishable structures are crescent membranes comprising a single lipoprotein bilayer with an external honeycomb lattice composed of trimers of the D13 protein (2–5). The crescents enclose adjacent electron-dense material containing core proteins and a DNA nucleoid to form the spherical immature virion (IV). During subsequent stages of morphogenesis, the D13 scaffold is disrupted (6), major core proteins are cleaved (7), and some membrane proteins acquire intramolecular disulfide bonds (8), resulting in brick-shaped infectious mature virions (MVs). Some MVs are wrapped by the *trans*-Golgi network or endosomal cisternae (9–11) and are transported by microtubules to the plasma membrane, where exocytosis occurs, allowing the enveloped virions to spread to neighboring cells (12, 13).

There have been contradictory theories about the origin of the poxvirus membrane, including *de novo* synthesis (14) and recruitment of the intermediate compartment between the endoplasmic reticulum (ER) and the Golgi apparatus (15). Recent reports suggest that the crescent membrane is derived from the ER (16–21), although the mechanism involved remains to be determined and other models of viral membrane formation have not been excluded. Combined genetic and microscopic approaches are increasing our understanding of the process. Studies with conditional lethal mutants have identified several VACV proteins with dedicated roles in crescent membrane formation. These include A17 (22–24), A14 (24–26), F10 (27–29), A11 (30, 31), H7 (32), L2 (33), and A6 (34). In the absence of these proteins, dense masses of viroplasm and, in some cases, vesicles or tubules accumulate instead of crescents and IVs. Repressed synthesis of the scaffold protein D13 or addition of the drug rifampin has a quite different

effect: irregular membrane sheets surround electron-dense viroplasm (35–38). The A17 and A14 transmembrane (TM) proteins are likely structural elements, since they are components of both the IV and MV membranes. F10 (39) and A6 (34), in contrast to A17 and A14, are resistant to detergent extraction and remain associated with the core of the MV; A11, H7, and L2 are absent or present at very low concentrations in purified MVs. L2 has several unique characteristics—early expression, colocalization with the ER throughout the cytoplasm, and presence at the edges of the crescent membranes—that differentiate it from the other proteins in the group (19, 33). In addition, images suggesting continuity between modified ER membranes and IV-like structures have been obtained for cells infected with an L2 deletion mutant (20).

The major purpose of the present study was to investigate the intracellular localization of A11 in infected cells in order to find clues regarding its enigmatic role in the formation of IV membranes. The first reference to the A11 protein was the report of its association with the VACV DNA packaging protein A32 in a yeast two-hybrid screen (40). Although that interaction was confirmed by weak coimmunoprecipitation from infected cells (30), the significance of this association remains obscure. Our laboratory reported (30) that A11 is expressed late in infection with an apparent mass of 40 kDa, is not associated in significant amounts with purified MVs, is phosphorylated independently of the VACV F10 protein kinase, localizes in cytoplasmic viral factories, and self-

Received 12 June 2013 Accepted 3 July 2013

Published ahead of print 17 July 2013

Address correspondence to Bernard Moss, bmoss@nih.gov.

Copyright © 2013, American Society for Microbiology. All Rights Reserved.

doi:10.1128/JVI.01601-13

associates to form dimers or higher-order structures. When the expression of A11 was repressed, there was a specific block in morphogenesis resulting in the accumulation of large, dense bodies containing core proteins (30), a phenotype similar to those subsequently described for H7 (32), L2 (19), and A6 (34) mutants. Although the A11 protein is predicted to have TM domains, the Triton X-114 (TX-114)-solubilized protein partitioned largely in the aqueous phase, suggesting that A11 is not sufficiently hydrophobic to be an integral membrane protein (30). However, the recent demonstration that L2 is ER associated (19) provided the impetus for the present experiments. While our studies were well under way, Wu and coworkers (31) reported that A11 interacts weakly with A6, partitions equally into TX-114 and aqueous phases, and associates with viral membranes in factories when A6 is expressed. However, in neither the original (30) nor the more recent (31) report were cellular organelle markers used in fluorescence microscopy, or antibodies to A11 in electron microscopy, to identify the viral or cellular structures associated with A11.

Here we report that A11 has both similar and distinctive features compared to L2. A11 colocalized with the ER within virus factories instead of throughout the cytoplasm, as occurs with L2. However, A11, like L2, was present at the edges of crescent viral membranes during a normal infection and was located on or near aberrant membranes in cells infected with mutant viruses. In uninfected cells, A11 did not colocalize with the ER or associate with membranes, as did L2, even when L2, A6, or H7 was coexpressed. *In vitro* transcription and translation experiments indicated that both A11 and L2 are tail-anchored proteins that associate post-translationally with microsomal membranes. When the expression of A11 was repressed during infection, in addition to the large, dense bodies that are also found in infections with H7 and A6 mutants, we detected IV-like structures adjacent to the ER, which had previously been seen only with an L2 deletion mutant (20).

MATERIALS AND METHODS

Cells and virus. BS-C-1, RK-13, and HeLa cells were grown in minimum essential medium with Earle's salts (E-MEM) and in Dulbecco's minimum essential medium (DMEM), supplemented with 10% fetal bovine serum (FBS), 100 U of penicillin, and 100 µg of streptomycin per ml (Quality Biologicals, Gaithersburg, MD). The medium of RK-13 cells stably expressing calnexin with a V5 epitope tag was supplemented with 300 µg/ml Zeocin (20). The VACV Western Reserve (WR) strain and the recombinant viruses vL2-HA (19), vA9-HA (41), vA6L-V5 (34), vFS-H7 (32), vA17LΔ5 (22), vindA14 (26), and vA11Ri (30) were propagated as described previously (42).

Antibodies. The following antibodies were used to detect epitope tags: an anti-HA.11 mouse monoclonal antibody (MAb) (Covance, Denver, PA), an anti-FLAG M2 mouse MAb (Sigma-Aldrich, St. Louis, MO), and an anti-V5 mouse MAb (Pierce; Thermo Scientific). For the detection of VACV proteins, rabbit antisera to A17-N (43), A11 (30), A3 (unpublished data), and D13 (B1) (38) and a mouse MAb to A11 (31) were used. For the detection of cellular proteins, goat polyclonal IgG to protein disulfide isomerase (PDI) (Santa Cruz Biotechnology), an anti-calnexin rabbit antibody (Covance, Emeryville, CA), and an anti-calnexin mouse MAb (Pierce; Thermo Scientific) were used.

Confocal microscopy. HeLa cells grown on coverslips were infected with VACV, fixed with 4% paraformaldehyde in phosphate-buffered saline (PBS) for 15 min at room temperature, and washed with PBS. The cells were permeabilized for 15 min with 0.1% Triton X-100 in PBS at room temperature and were blocked with 10% FBS for 30 min. After blocking, the cells were incubated with the primary antibody in PBS con-

taining 10% FBS for 1 h at room temperature. Cells were washed and were incubated with the secondary antibody conjugated to a dye (Molecular Probes, Eugene, OR) for 1 h. The coverslips were incubated for 10 min with 300 nM 4',6-diamidino-2-phenylindole (DAPI; Invitrogen Life Technologies) in PBS, washed, and mounted on a glass slide by using ProLong Gold (Invitrogen Life Technologies). Micrographs were acquired with a Leica TCS SP5 confocal inverted-base microscope with a 63× oil objective. Images were analyzed by Leica LAS AF, Huygens, and Imaris X64 7.6.1 (Bitplane Scientific Software). At least 10 cells were analyzed for each treatment. The colocalization of fluorophores was quantified using Imaris X64 7.6.1, Pearson's correlation coefficient, and Manders' overlap coefficient (44).

Plasmid construction. The A11R, A6L, H7R, and L2R open reading frames (ORFs) from VACV WR, codon optimized for mammalian expression, were synthesized by GeneArt Life Technologies (Carlsbad, CA) and were cloned into the pMK plasmid. The plasmids were used as templates for preparing copies of the ORFs by PCR, and the products were transferred into pcDNA 3.1D/V5-His-TOPO (Invitrogen Life Technologies). The C-terminal A11 deletion mutant (A11-ΔCt) was generated by using the A11 plasmid mentioned above as a template, and oligonucleotides were generated to delete the C-terminal 204 nucleotides from the A11 ORF. The PCR product was also inserted into plasmid pcDNA 3.1D/V5-His-TOPO.

Transfection studies. HeLa cells were grown on coverslips in 24-well plates. After reaching 80% confluence, the cells were transfected by using Lipofectamine 2000 (Invitrogen Life Sciences) according to the instructions of the provider. The cells received fresh medium at 6 h posttransfection. After 24 h, the cells were fixed and prepared for confocal microscopy.

Subcellular fractionation. The procedure for subcellular fractionation was modified from alternate protocol 2 of Graham (45). HeLa cells in a 3- by 100-mm culture dish were infected or transfected. Subsequently, the medium was replaced with cold homogenization buffer (0.25 M sucrose, 10 mM Tris-HCl [pH 7.4], 1 mM EDTA, protease inhibitor cocktail tablets [Roche Diagnostics]). After 10 min on ice, the cells were scraped and were centrifuged for 10 min at 2,000 × g and 4°C. The cells were washed with homogenization buffer and were disrupted by 30 strokes of a Dounce homogenizer with a loose-fitting pestle. The lysate was cleared by centrifugation in the cold for 20 min at 2,000 × g. The supernatant was loaded at the bottom of a preformed 0-to-35% continuous iodixanol gradient (Sigma-Aldrich) and was centrifuged at 200,000 × g for 3 h at 4°C. After centrifugation, 0.5-ml fractions were collected using a Piston Gradient Fractionator (BioComp Instruments). Proteins in each fraction were analyzed by electrophoresis on 4-to-12% Novex NuPAGE acrylamide gels followed by Western blotting.

In vitro transcription and translation. The TNT coupled reticulocyte lysate system (Promega) was used for *in vitro* transcription/translation as directed by the manufacturer. Briefly, 12.5 µl TNT lysate, 0.5 µl TNT reaction buffer, 20 µM amino acid mixture minus methionine, 20 U RNasin RNase inhibitor, 0.5 µl TNT T7 RNA polymerase, 20 µCi [³⁵S]methionine, 1 µg plasmid, and 2.5 µl canine microsomal membranes were mixed in a 25-µl final volume. After 60 min at 30°C, the reaction mixtures were centrifuged for 20 min at full speed in a microcentrifuge. The supernatant was recovered and was kept on ice. In order to remove proteins loosely bound to the microsomes, the pellet was suspended in 0.2 ml of PBS and was recentrifuged. The pellets were suspended in 50 µl of PBS, layered on top of 75 µl of 0.5 M sucrose, and centrifuged at full speed for 20 min (46). The microsome-associated protein was then analyzed by sodium dodecyl sulfate-polyacrylamide gel electrophoresis (SDS-PAGE). The gels were dried and were imaged using a Kodak storage phosphor screen with an exposure cassette (Amersham Biosciences).

Before layering onto 0.5 M sucrose, some samples were treated with 0.5 mg of proteinase K (Invitrogen)/ml for 1 min in the absence or presence of 1% Triton X-100 detergent at room temperature. In some experiments, the pellets were incubated in 0.1 ml of Na₂CO₃ (pH 11), kept on

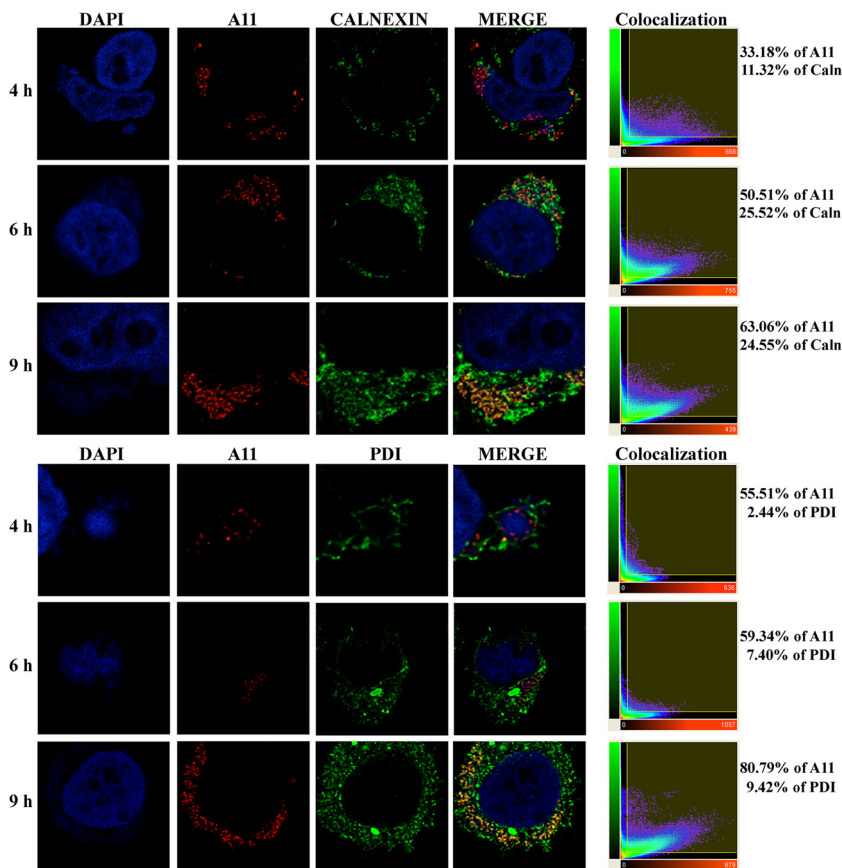


FIG 1 Colocalization of A11 with ER marker proteins. HeLa cells were infected with vL2-HA at a multiplicity of 3 PFU per cell. After 4, 6, and 9 h, the infected cells were fixed, permeabilized, and stained with a rabbit polyclonal antibody to A11 and a mouse MAb to the cellular ER protein calnexin or PDI, followed by goat anti-rabbit IgG and goat anti-mouse IgG coupled to Alexa Fluor 594 and Alexa Fluor 647, respectively. Nuclei and viral factories were stained with DAPI. Individual and merged confocal microscopic images are shown in the four panels on the left, and colocalization scatter plots are shown on the right. Colocalization values, expressed as percentages, are given.

ice for 20 min, and then centrifuged again. In order to investigate post-translational membrane insertion, transcription and translation reactions were carried out in the absence of microsomal membranes. Then 200 µg/ml of cycloheximide was added to block further translation, and 2.5 µl of microsomal membranes was added. After 30 min at 30°C, the membranes were collected, washed, and analyzed as described above.

Transmission electron microscopy. Infected BSC-1 cells or RK-13 cells stably expressing calnexin with a V5 epitope tag in 60-mm-diameter wells were prepared for cryosectioning and immunogold labeling as described previously (47). Cryosections were picked up on grids, thawed, washed free of sucrose, and stained with an anti-A17, anti-A11, or anti-D13 polyclonal antibody or a mouse MAb to the V5 or hemagglutinin (HA) epitope, followed first by rabbit anti-mouse IgG from Cappel, ICN Pharmaceuticals (Aurora, OH) and then by protein A conjugated to 10-nm gold spheres (University Medical Center, Utrecht, Netherlands). Double labeling with 5- and 10-nm gold spheres was carried out as described previously (6). Specimens were viewed with a FEI Tecnai Spirit transmission electron microscope (FEI, Hillsboro, OR).

RESULTS

Colocalization of A11 with the ER and L2 protein. A hydrophobicity plot of A11 predicted two TM domains within the C-terminal 77 amino acids, followed by a short, positively charged tail (30). To investigate the membrane association of A11, HeLa cells were infected with VACV, and at various times, the cells were fixed

and incubated with a polyclonal antibody to the A11 protein. DAPI was used to stain DNA in the nucleus and adjacent cytoplasmic virus factories; the ER was visualized by staining with antibodies specific for the ER integral membrane protein calnexin or the ER luminal protein PDI (Fig. 1). A11 localized primarily within virus factories, where viral DNA and late proteins are synthesized and virus particles assembled. Visual inspection suggested that some ER was present in virus factories, where it colocalized with A11 (Fig. 1). This impression was corroborated by automated quantitative determination of colocalization coefficients (44). The colocalization of A11 with calnexin increased from 33% at 3 h to 63% at 9 h, as shown in scatter plots (Fig. 1). The colocalization of calnexin with A11 increased from 11% at 3 h to 25% at 6 and 9 h. The lower percentage of calnexin colocalizing with A11, compared to the reverse, results from the location of calnexin outside as well as inside the factory. Similar results were obtained by comparing A11 and PDI: the colocalization of A11 with PDI increased from 56% at 3 h to 81% at 9 h postinfection (Fig. 1). The low level of PDI colocalizing with A11 was also attributed to the presence of the majority of this luminal protein in the ER outside the factory.

The L2 protein, which is also predicted to have two TM domains near the C terminus, has been shown previously to colocalize with the ER both within and outside the virus factory (19). It

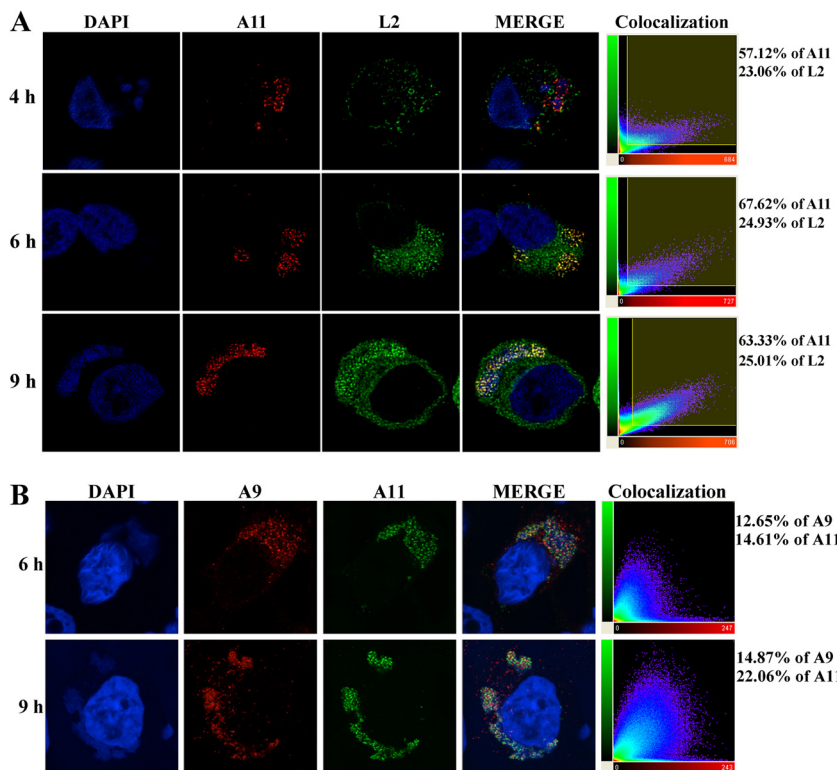


FIG 2 Colocalization of A11 with viral proteins. (A) Colocalization of A11 with L2. HeLa cells were infected with vL2-HA at a multiplicity of 3 PFU per cell. After 4, 6, and 9 h, the infected cells were fixed, permeabilized, and stained with a rabbit polyclonal antibody to A11 and a mouse MAb to the HA epitope tag attached to L2, followed by goat anti-rabbit IgG and goat anti-mouse IgG coupled to Alexa Fluor 594 and Alexa Fluor 647, respectively. Nuclei and virus factories were stained with DAPI. (B) Colocalization of A11 with A9. HeLa cells were infected with vA9-HA at a multiplicity of 3 PFU per cell. After 6 and 9 h, the infected cells were prepared for confocal microscopy and were stained with the polyclonal antibody to A11 and a mouse MAb to the HA tag of A9. The same secondary antibodies were used as for panel A. Confocal microscopy and colocalization were performed as for Fig. 1.

was therefore of interest to determine the colocalization of A11 with L2. The extent of colocalization was 57% at 3 h and increased slightly, to >60%, at later times (Fig. 2A). Because of its presence outside factories, only 25% of L2 colocalized with A11. To be sure that the strong colocalization of A11 with L2 was not due simply to their presence in the virus factory, we also compared A11 with A9, which is associated mostly with MV membranes (41). Despite the fact that both A11 and A9 were located in the viral factory, there was a notable distinction between the areas that they occupied (Fig. 2B). A11 colocalization with A9 increased to only 22%, considerably less than the 63% colocalization obtained with L2, and only 15% of A9 colocalized with A11.

Intracellular localization of A6 and H7. We were interested in using quantitative confocal microscopy to compare the intracellular localization of A6 and H7, which play roles in crescent formation but do not have transmembrane domains like A11 and L2 and are distributed throughout the cell (32, 34). HeLa cells were infected with a recombinant VACV containing either V5-tagged A6 or FLAG-tagged H7, fixed, and stained with a MAb to the V5 or FLAG epitope and a polyclonal antibody to calnexin. A6 localized throughout the cytoplasm, although it was also associated with viral factories, particularly at the earlier times (Fig. 3). The colocalization of A6 with calnexin increased slightly, from 49% at 4 and 6 h to 53% at 9 h. The colocalization of calnexin with A6, however, increased from 27% to 56% concomitantly with the increasing cytoplasmic distribution of A6. Although H7 was also

distributed throughout the cell, only 16% of H7 colocalized with calnexin and 18% of calnexin colocalized with H7 (Fig. 3). We concluded that A6, but not H7, colocalized extensively with the ER.

Localization of A11 in uninfected cells. Transfection experiments were carried out to determine the localization of A11 in uninfected HeLa cells. In contrast to the images of infected cells, A11 appeared to have a broad cytoplasmic distribution and in some cells was concentrated in the subcortical area (Fig. 4). There was little or no colocalization with either calnexin (Fig. 4) or actin (not shown). This result contrasts with the ER localization of L2 when expressed by transfection in uninfected cells (19). To explore the possibility that interactions with other viral proteins are needed for A11 to localize with the ER, we cotransfected the plasmid encoding A11 with a plasmid encoding L2, A6, or H7. However, the colocalization of A11 with calnexin was not substantially increased by coexpression with any of these proteins (Fig. 4), and only about 30% of A11 colocalized with A6 and 10 to 15% with L2 and H7 (not shown). It is possible that other viral proteins or expression within the virus factory is needed for A11 to localize with the ER.

Subcellular fractionation of A11. An independent method was used to evaluate the extent to which A11 associated with membranes in infected and uninfected cells. Cell lysates were loaded at the bottoms of preformed iodixanol gradients, allowing membranes to float upward during centrifugation depending on

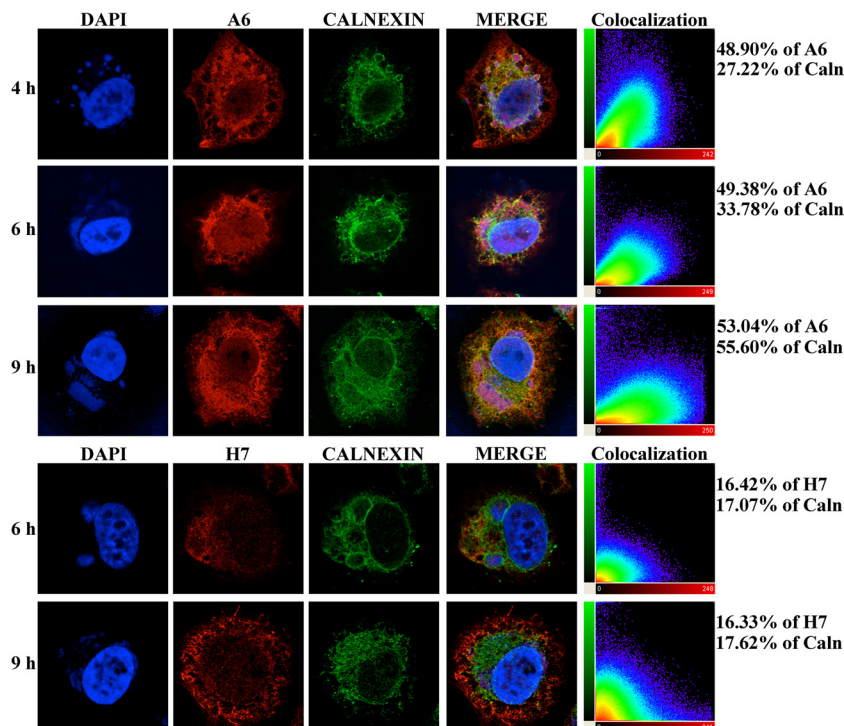


FIG 3 Colocalization of A6 and H7 with calnexin. HeLa cells were infected with vA6-V5 or vH7-FLAG at a multiplicity of 3 PFU per cell. After 4, 6, and 9 h, the infected cells were fixed, permeabilized, and stained with a rabbit polyclonal antibody to calnexin and a mouse MAb to the V5 or FLAG epitope fused to A6 or H7, respectively. This step was followed by goat anti-rabbit IgG and goat anti-mouse IgG coupled to Alexa Fluor 594 and Alexa Fluor 647, respectively. Nuclei and virus factories were stained with DAPI. Confocal microscopy and colocalization analyses were carried out as for Fig. 1.

their density. Fractions from the gradients were analyzed by Western blotting using antibodies to cellular ER and cytoskeletal proteins calnexin and α -actinin, respectively, and to the viral proteins A11, L2, and A3. The latter is a component of the virus core. In the sample from infected cells, L2 closely tracked the ER marker calnexin, as expected from confocal microscopy. A11 was in membrane fractions corresponding to heavier calnexin and L2 fractions that were presumably derived from factories, whereas A3 was in the still heavier virion fractions (Fig. 5). In contrast, A11 from uninfected cells remained near the bottom of the tube, indicating little or no membrane association (Fig. 5). Thus, the subcellular fractionation analysis was consistent with the confocal microscopy data and demonstrated that A11 was specifically associated with membranes in infected cells but not in uninfected cells.

Association of A11 with microsomal membranes *in vitro*. The failure of A11 to colocalize with the ER in uninfected cells led us to try an alternative approach to ascertaining whether A11 has an intrinsic ability to associate with the ER. When a DNA template-encoding A11 was transcribed and translated in a reticulocyte lysate in the presence of microsomes, the radioactively labeled protein of the expected length, as well as smaller products, was detected in both soluble and sucrose cushion-purified membrane pellet fractions (Fig. 6A). Control experiments showed that these proteins were not detected in the absence of the DNA template or when other templates were used (Fig. 6A) and were entirely in the soluble fraction when microsomes were omitted (Fig. 6B). Similarly, a protein of the size predicted for L2 was made using an L2-specific template and was detected in soluble and pellet fractions (Fig. 6A), and both A11 and L2 proteins were made when the

two DNA templates were transcribed and translated in the same reaction (Fig. 6A). The diffuse band in the soluble fraction just above L2 is hemoglobin, which was removed during pelleting through the sucrose cushion. The membrane-bound A11 was resistant to treatment with Na_2CO_3 , which removes peripherally bound proteins (Fig. 6B). The proteinase sensitivity of A11, without or with detergent, suggested that A11 was oriented with the long N-terminal domain outside the microsomes (Fig. 6B). Thus, A11 was able to associate with microsomes in this *in vitro* system in the absence of other viral proteins.

Many proteins with C-terminal TM domains, such as VACV H3 (46), are tail anchored and are inserted posttranslationally into microsomal membranes (48). To determine whether A11 and L2 can be inserted posttranslationally, the proteins were first synthesized in the reticulocyte extract, and then cycloheximide (to prevent further synthesis of A11 and L2) and microsomes were added. Both A11 and L2 pelleted with microsomes under these conditions (Fig. 6C), indicating posttranslational membrane insertion. To determine the nucleoside triphosphate requirement for the posttranslational insertion of A11 and L2 into microsomes, the extracts were passed through gel filtration columns before the addition of microsomes. The association of A11 and L2 with microsomes was only partially decreased under our conditions. Further studies would be needed to evaluate the mechanism of insertion and to determine whether specific chaperones are involved.

The effect of deletion of the C-terminal hydrophobic domain on the ability of A11 to associate with microsomes was determined. The truncated A11 protein was in the soluble fraction in the absence and presence of microsomes (data not shown), confirming the location of

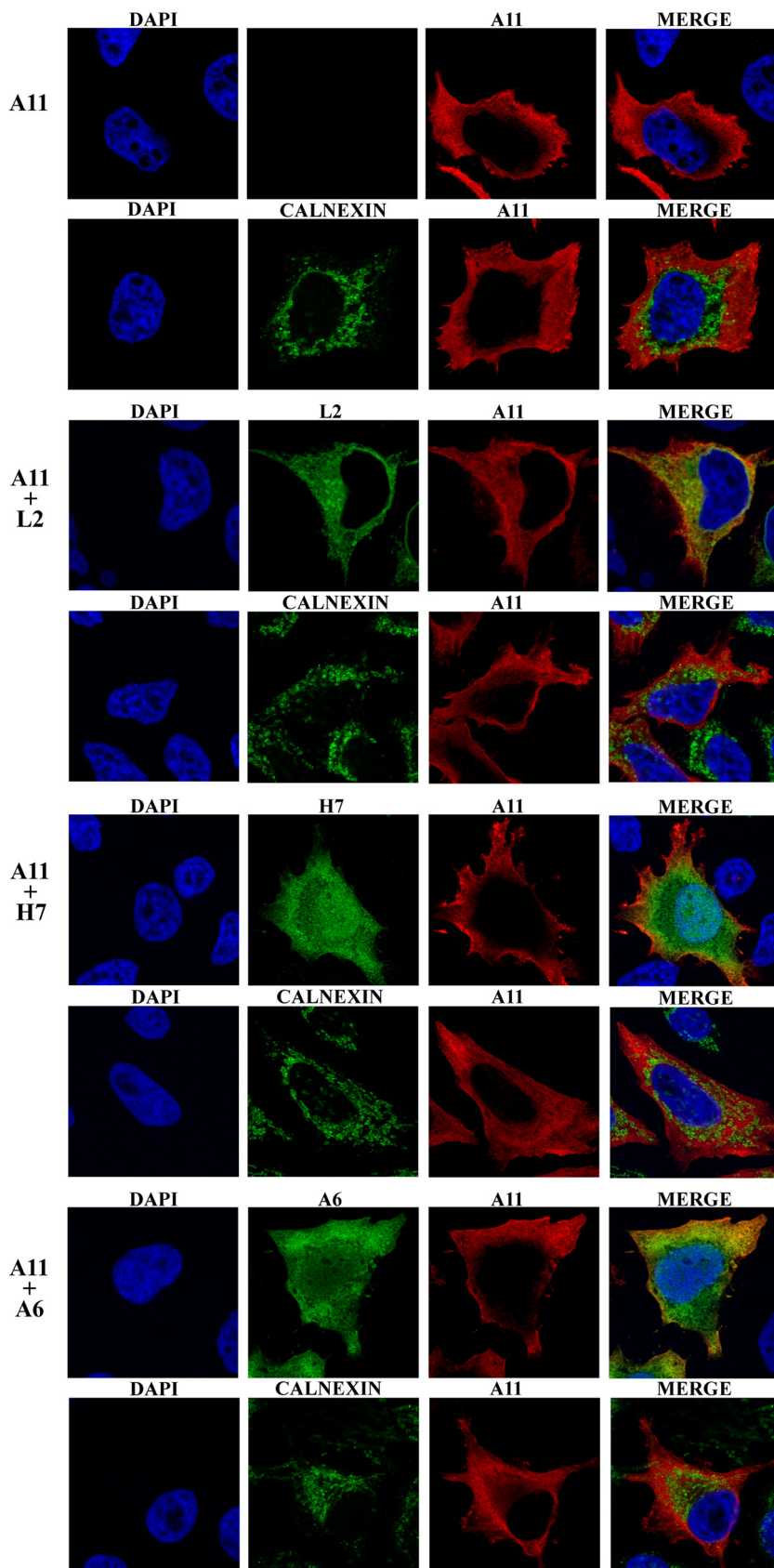


FIG 4 Localization of A11 in uninfected cells in the absence and presence of L2, H7, or A6. HeLa cells were transfected for 30 h with a combination of plasmids expressing A11, L2-HA, H7-HA, and A6-V5, as indicated, regulated by the cytomegalovirus promoter. The cells were fixed, permeabilized, and stained with a rabbit polyclonal antibody to A11 and with a mouse MAb to the HA epitope tag attached to L2 or H7, the V5 epitope attached to A6, or calnexin, followed by goat anti-mouse IgG coupled to Alexa Fluor 488 and goat anti-rabbit IgG coupled to Alexa Fluor 594. Nuclei were stained with DAPI.

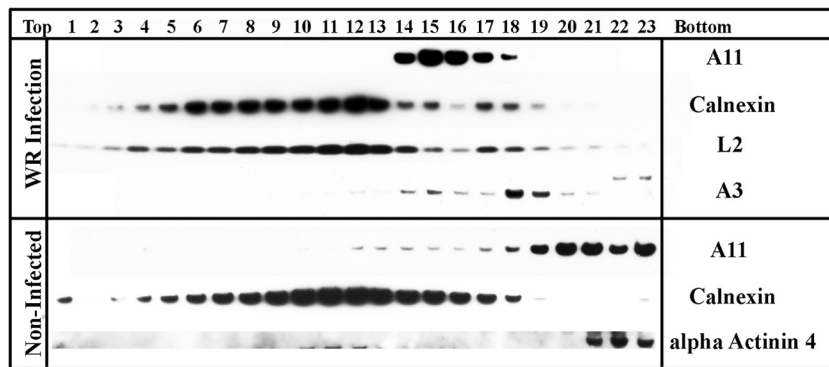


FIG 5 Subcellular fractionation of A11 in infected and uninfected cells. HeLa cells either were infected with VACV strain WR at a multiplicity of 5 PFU per cell for 16 h or were transfected with a plasmid expressing codon-optimized A11 under the control of the cytomegalovirus promoter for 48 h. The cells were lysed and were layered under a iodixanol gradient. After centrifugation, 23 fractions were collected from each gradient and were analyzed by Western blotting using the antibodies indicated. The top and bottom of the gradient are indicated.

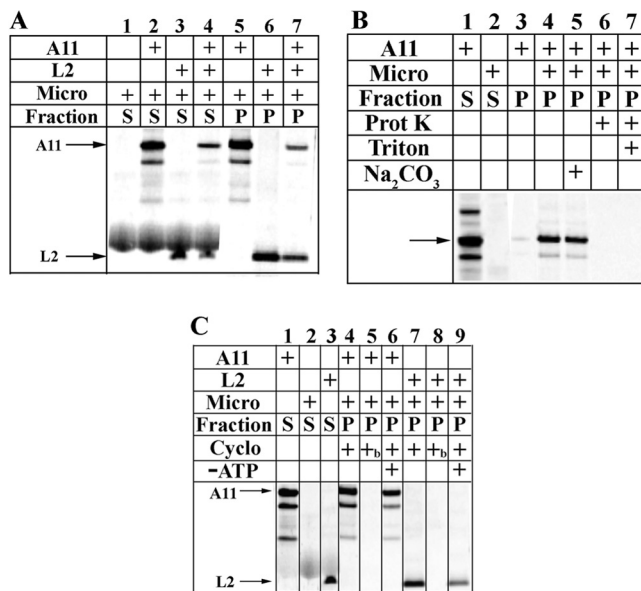


FIG 6 Cell-free synthesis of A11 and L2 proteins. (A) Association of A11 and L2 with microsomal membranes. The A11 and L2 ORFs were transcribed from a DNA template and were translated in a reticulocyte cell-free system with [³⁵S]methionine in the presence of canine microsomal membranes (Micro). The mixtures were layered over a sucrose cushion and were centrifuged to separate the supernatant (S) and microsome-associated pellet (P) fractions. The samples were analyzed by SDS-PAGE and autoradiography. Arrows indicate full-length A11 and L2 proteins. (B) Na₂CO₃ resistance and proteinase sensitivity of membrane-associated A11. The A11 ORF was transcribed and translated in the presence or absence of microsomal membranes, and supernatant and pellet fractions were obtained as for panel A. Pellet fractions were treated either with proteinase K (Prot K) alone for 1 min (lane 6) or with Triton X-100 (Triton) plus proteinase K (lane 7). For lane 5, the pellet was resuspended in Na₂CO₃ and was centrifuged again. The arrow points to the full-length A11 protein. (C) Posttranslational insertion of the A11 and L2 proteins into membranes. Transcription and translation in the absence or presence of DNA encoding A11 or microsomal membranes was carried out as described for panel A. Cycloheximide (Cyclo) was added at the start of the reaction (+_b) to demonstrate complete inhibition of translation (lanes 5 and 8) or just before the addition of microsomal membranes (+) (lanes 4, 6, 7, and 9). For lanes 6 and 9, the reaction mixture was passed through a Sephadex G-50 column prior to the addition of microsomes to partially deplete ATP (-ATP). Arrows indicate the positions of the A11 and L2 proteins.

the TM domain. Moreover, the membrane association of the truncated A11 could not be rescued by cosynthesis of full-length L2 (data not shown), suggesting the absence of a strong interaction between the N-terminal domain of A11 and L2.

Association of A11 with viral membranes. Transmission electron microscopy was used to visualize the association of A11 with viral membranes in the factory. We used a recombinant virus expressing epitope-tagged L2 in order to also visualize the latter. Cryosections from cells infected with vL2-HA were either stained with a polyclonal antibody to A11 followed by protein A conjugated to 10-nm gold spheres (Fig. 7A and B) or with an anti-HA MAb followed by an anti-mouse MAb and protein A conjugated to 5-nm gold spheres, to detect L2 (not shown), or were double labeled to detect both A11 and L2 (Fig. 7C and D). A11 was detected on membranes near and associated with crescents and IVs (Fig. 7A to D). By counting random cell sections, we estimated that similar numbers of IVs and crescents were labeled with the antibody to A11. One or more gold grains were found near the ends of nearly all crescents and open IVs, but they were also present at other regions along the membranes. L2 had a localization similar to that shown previously (19).

Additional experiments were carried out to localize A11 in cells infected with A17 and A14 conditional lethal null mutants under nonpermissive conditions. When the expression of either protein is repressed, large numbers of vesicles and tubules form instead of IVs near large, dense masses of viroplasm (22, 23, 25, 26). Due to the inability of antibodies to penetrate these dense inclusions after fixation, core proteins, such as A3, are visualized by confocal microscopy as circles within the cytoplasm (Fig. 8), as shown previously (33). The antibody to the A11 protein appeared as overlapping circles (Fig. 8), indicating association with the inclusions.

Immunoelectron microscopy of thin cryosections was used to more precisely localize A11 in the absence of A14 and A17. A11 was detected near the vesicles and tubules formed when A17 (Fig. 9A) or A14 (Fig. 9B) was repressed, further supporting viral membrane association. Similar staining was detected for L2 (Fig. 9C and D). Double-label experiments confirmed the similar locations of A11 and L2 (Fig. 9E and F).

Formation of aberrant IV-like membranes when A11 synthesis is repressed. Previously, we showed that large, dense viroplasmic aggregates formed when the synthesis of A11 was repressed

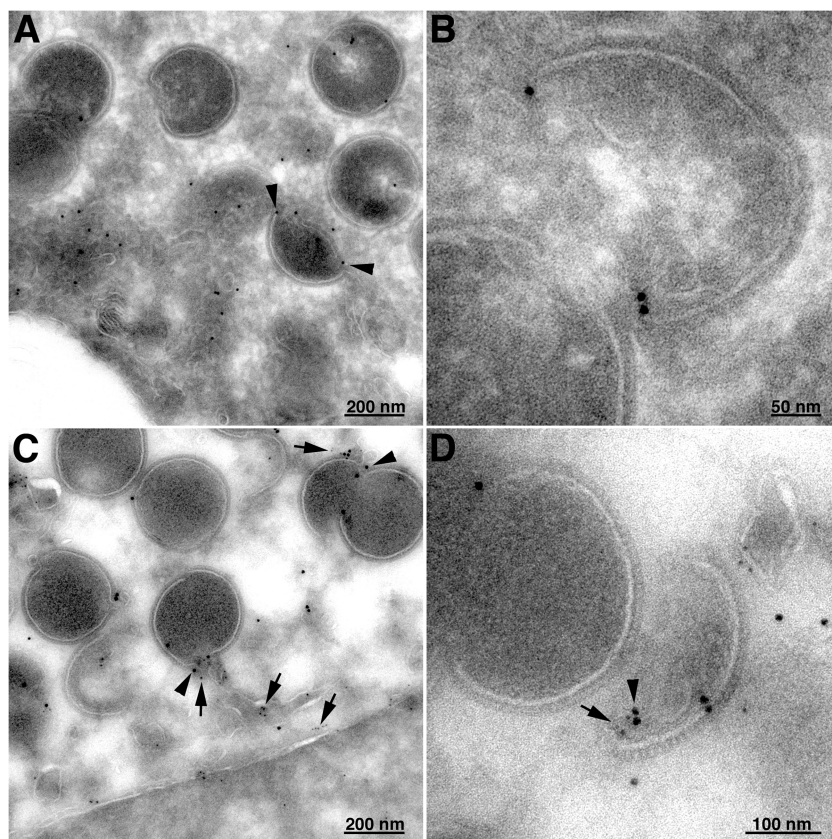


FIG 7 Localization of A11 and L2 by immunogold transmission electron microscopy. BS-C-1 cells were infected with vL2-HA at a multiplicity of 5 PFU per cell. After 9 h, the cells were fixed, cryosectioned, and either incubated with a rabbit antibody to A11 (A and B) or double labeled with a rabbit antibody to A11 and a mouse MAb to the HA tag fused to L2 (C and D). A11 is bound to 10-nm gold spheres (arrowheads); L2 is bound to 5-nm gold spheres (arrows).

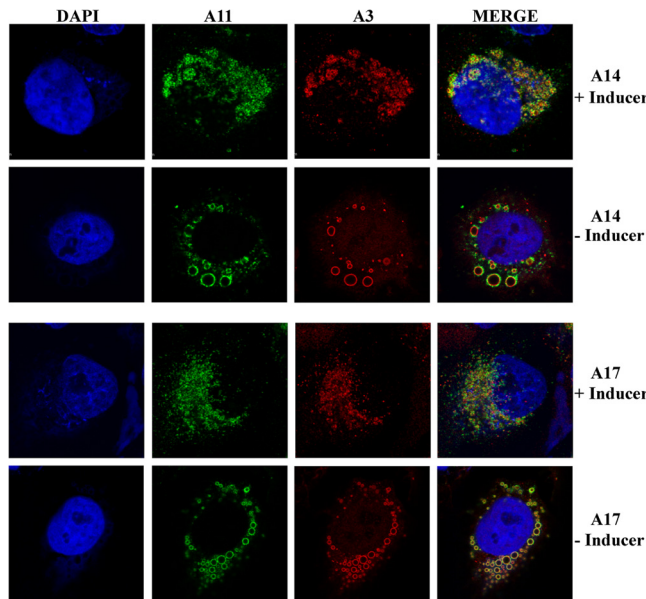


FIG 8 Localization of A11 by confocal microscopy in the absence of A17 or A14. HeLa cells were infected with A17-inducible VACV or A14-inducible VACV at a multiplicity of 3 PFU per cell in the presence (+) or absence (-) of 100 μ M isopropyl- β -D-thiogalactopyranoside or 1 μ g per ml of tetracycline, respectively. After 16 h, the infected cells were fixed, permeabilized, and stained with rabbit polyclonal and mouse monoclonal antibodies to A3 and A11 followed by goat anti-rabbit IgG and goat anti-mouse IgG coupled to Alexa Fluor 594 and Alexa Fluor 488, respectively. Nuclei and virus factories were stained with DAPI.

during the infection of BS-C-1 cells (30). In the present study, using RK-13 cells, IV-like structures that appeared relatively empty of viroplasm were found in addition to the dense aggregates (Fig. 10A). The membranes were coated with spicules (shown at a higher magnification in the Fig. 10A inset), indicating the presence of the D13 scaffold (5). In RK-13 cells, these IV-like structures were seen as frequently as the masses of dense viroplasm, whereas IV-like structures were uncommon in BS-C-1 cells, accounting for our previous failure to describe them (30). These aberrant structures were reminiscent of those seen in BS-C-1 and RK-13 cells infected with an L2 deletion mutant (20). D13 was detected on the surfaces of the IV-like structures by immunoelectron microscopy of cryosections (Fig. 10B). A17 was also identified in the membranes of the IV-like structures (Fig. 10C). Furthermore, using an RK-13 cell line stably transfected with V5 epitope-tagged calnexin (20), we detected ER membrane intimately associated with the IV-like structures (Fig. 10D).

DISCUSSION

The initial VACV membrane consists of a single bilayer whose convex surface is coated with a spicule or honeycomb lattice (3–5, 14, 18, 49). Genetic studies have identified a number of viral proteins required for the early stages of virion assembly. Detailed characterization of these proteins and the effects of conditional lethal mutants are providing important insights into viral membrane biogenesis. The purpose of the present study was to further

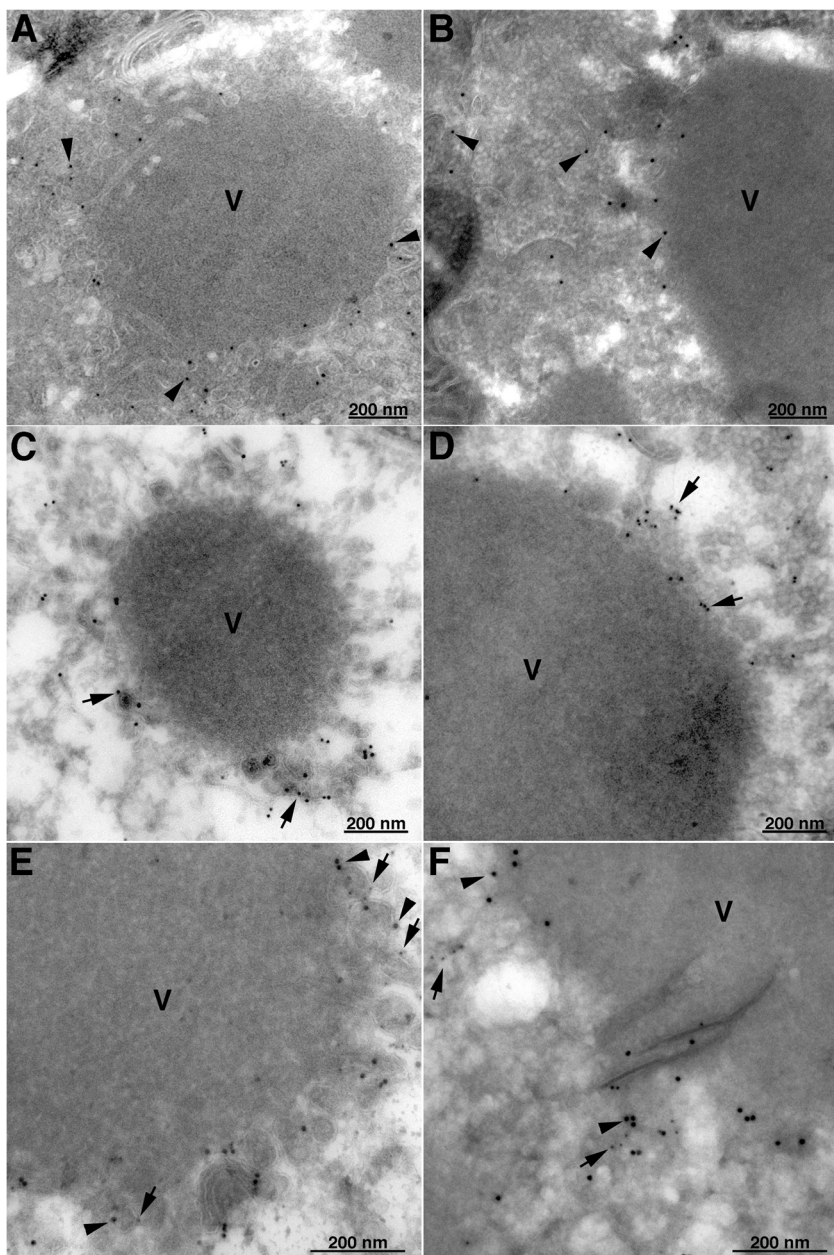


FIG 9 Localization of A11 and L2 in the absence of A17 or A14 by transmission electron microscopy. BSC-1 cells were infected with A17-inducible VACV (A, C, and E) or A14-inducible VACV (B, D, and F) in the absence of an inducer. For panels C to F, cells were also transfected with a plasmid that expresses the L2 protein with an N-terminal HA tag regulated by the natural promoter. After 20 h, the cells were fixed, cryosectioned, and either stained with a rabbit antibody to A11 followed by protein A conjugated to 10-nm gold spheres (A and B) or with a MAb to HA followed by rabbit anti-mouse IgG and protein A conjugated to 10-nm gold spheres (C and D) or double labeled with 10-nm gold spheres for A11 (arrowheads) and 5-nm gold spheres for L2 (arrows) (E and F). V, dense viroplasm.

characterize the VACV A11 protein, a nonvirion protein that had previously been shown to be required for the formation of IVs. Neither the original study (30) nor a very recent follow-up (31) had identified cellular organelles or viral structures associated with A11. Here we demonstrate that A11 is associated with the ER and immature viral membranes within viral factories. Furthermore, when A11 expression was repressed, there were aberrant IV-like structures closely associated with the ER in addition to previously described masses of viroplasm. The IV-like structures

were more abundant in infected RK-13 cells than in infected BSC-1 cells. We can only speculate that this difference might be related to the greater accessibility of the ER within the factories of some cell lines.

Confocal microscopy was used to locate A11, as well as the L2, A6, and H7 viral proteins, with apparently related functions in morphogenesis. The distribution of the ER throughout the cytoplasm and the concentration of A11 within the virus factory made it important to employ a rigorous analysis to verify specific asso-

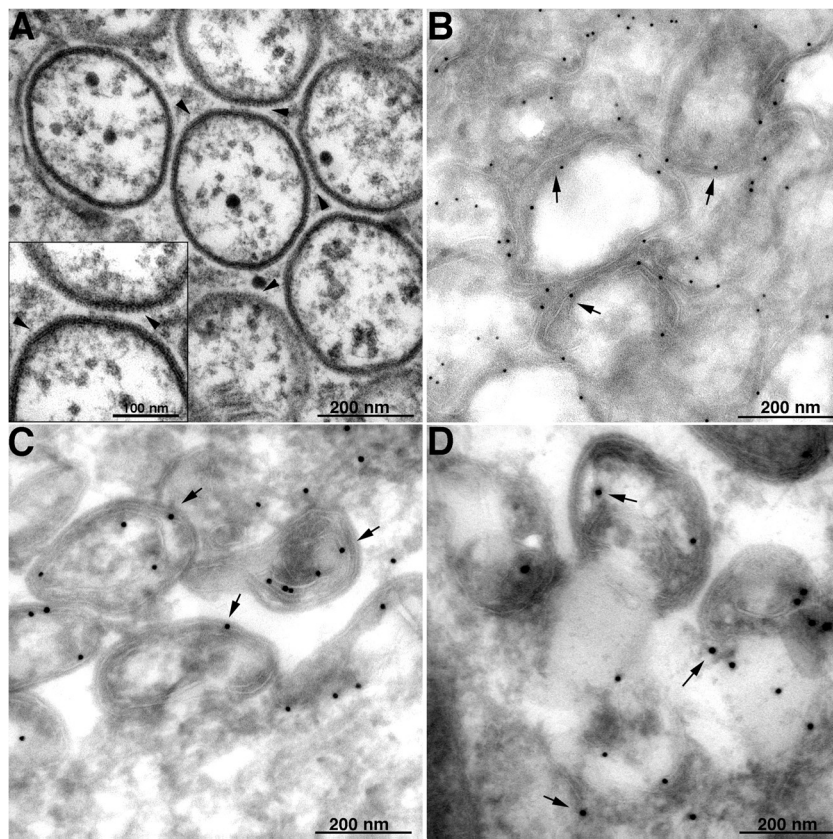


FIG 10 IV-like structures in the absence of A11. (A) RK-13 cells were infected with vA11Ri at a multiplicity of 10 PFU per cell in the absence of isopropyl- β -D-thiogalactopyranoside. After 24 h, the cells were fixed, embedded with Epon, and prepared for transmission electron microscopy. Arrowheads indicate the spicules of D13 covering the IV-like structures. (Inset) Higher magnification of the IV-like membrane. (B to D) RK-13 cells stably expressing V5-tagged calnexin were infected with vA11Ri at a multiplicity of 10 PFU per cell in the absence of isopropyl- β -D-thiogalactopyranoside. After 24 h, the cells were fixed, cryosectioned, and stained with a polyclonal antibody to D13 (B) or A17 (C) or with a MAb to the V5 tag fused to calnexin and with rabbit anti-mouse IgG (D) followed by protein A conjugated to 10-nm gold spheres. Arrows point to representative gold spheres.

cations. To avoid bias, we relied on an automated procedure to quantify overlaps in confocal microscopic images. Approximately 60 to 80% of A11 colocalized with the ER markers calnexin and PDI, respectively. A11 also colocalized to a similar extent with L2, which had been shown previously to associate with the ER. The finding that a much smaller amount of A11 colocalized with the A9 protein, which is associated mostly with MV membranes (41), served to validate our ability to resolve different structures within the virus factory. In addition, approximately 50% of the A6 protein colocalized with calnexin, whereas only 15% of H7 did. Thus, at least two and perhaps three of the four proteins with related roles in morphogenesis are ER associated. Since A6 does not have a predicted transmembrane domain, its association with the ER is likely to be indirect, possibly mediated by its weak association with A11 (31).

We determined previously that L2 associates with the ER in infected and uninfected cells, indicating that it occurs independently of any other viral protein (19). However, A11 did not colocalize with an ER marker and was distributed mostly near the cortices of uninfected cells. Coexpression of A6, L2, or H7 was insufficient to alter the localization of A11 in uninfected cells. Subcellular fractionation using iodixanol gradients was employed to determine whether A11 might have associated with other cellular membranes in uninfected cells. All of the A11 from the ly-

sates of infected cells floated up from the bottom of the tube to the density of the heavy ER. In contrast, A11 from the lysates of uninfected cells remained near the bottom of the tube, indicating a lack of membrane association.

Hydrophobicity plots of both A11 and L2 suggested the absence of a signal peptide and the presence of C-terminal TM domains, raising the possibility that these are tail-anchored proteins that use a posttranslational pathway to associate with the ER. Indeed, these predictions were fulfilled using an *in vitro* transcription/translation system that supported the insertion of both A11 and L2 into canine pancreatic microsomal membranes. In contrast to cotranslational ER membrane insertion, posttranslational insertion requires cytosolic chaperone complexes to shield the hydrophobic domains and target the proteins (48). In the absence of chaperones, tail-anchored proteins are subject to aggregation and mislocalization in cells (48, 50). Apparently, the conditions for the insertion of A11 into the ER membrane were met in infected but not uninfected HeLa cells. We noted that in infected cells, the amount of A11 associated with the ER greatly increased between 3 and 9 h after infection, implying delayed targeting. The report of Wu et al. (31) suggests that A6 may be one component of an A11 chaperone complex. It will be interesting to determine the mechanism of insertion of the A11 and L2 proteins into the ER.

Immunogold transmission electron microscopy indicated that

A11 associated with the edges of crescent membranes in addition to the ER, as previously shown for L2 (19). We further demonstrated that both A11 and L2 were associated with the abortive vesicles that formed when A14 or A17 synthesis was repressed. Despite their colocalization in infected cells, we have not been able to demonstrate a direct association between A11 and L2 by coimmunoprecipitation of extracts solubilized with a detergent. However, an interaction between A11 and A6 has been reported (31).

The localization of the A11 protein to the ER and immature viral membranes supports recent biochemical and microscopic data suggesting an ER origin for viral membranes (16–18, 20, 21). We propose a model in which L2 and A11, with the help of A6 and H7, participate in the recruitment of the ER to sites within the virus factory where morphogenesis occurs. This model can explain the aberrant structures that form when the synthesis of these proteins is repressed. Thus, short crescent membranes apposed to masses of dense viroplasm containing core proteins may accumulate when supplies of membrane at the assembly sites are limiting. In the absence of L2 and A11, some IV-like structures that lack viroplasm are also detected distal to assembly sites. These data suggest that individually, L2, A11, A6, and H7 may not be absolutely required for the conversion of the ER to abortive viral membranes. However, it would be interesting to determine the phenotype of a mutant unable to express combinations of the four proteins in order to rule out redundant functions.

ACKNOWLEDGMENTS

We thank our generous colleagues and coworkers, including Xiangzhi Meng and Yan Xiang of the University of Texas Health Center in San Antonio for vA6L-V5, Paula Traktman of the Medical College of Wisconsin for the A14-inducible virus, Catherine Cotter of the Laboratory of Viral Diseases, NIAID, for the preparation of cells, and Juraj Kabat of the Biological Imaging section, NIAID, for advice regarding quantitative colocalization imaging.

The research was supported by the Division of Intramural Research, NIAID, NIH.

REFERENCES

- Condit RC, Moussatche N, Traktman P. 2006. In a nutshell: structure and assembly of the vaccinia virion. *Adv. Virus Res.* 66:31–124.
- Dales S, Siminovitch L. 1961. The development of vaccinia virus in Earle's L strain cells as examined by electron microscopy. *J. Biophys. Biochem. Cytol.* 10:475–503.
- Hollinshead M, Vanderplasschen A, Smith GL, Vaux DJ. 1999. Vaccinia virus intracellular mature virions contain only one lipid membrane. *J. Virol.* 73:1503–1517.
- Heuser J. 2005. Deep-etch EM reveals that the early poxvirus envelope is a single membrane bilayer stabilized by a geodetic “honeycomb” surface coat. *J. Cell Biol.* 169:269–283.
- Szajner P, Weisberg AS, Lebowitz J, Heuser J, Moss B. 2005. External scaffold of spherical immature poxvirus particles is made of protein trimers, forming a honeycomb lattice. *J. Cell Biol.* 170:971–981.
- Bisht H, Weisberg AS, Szajner P, Moss B. 2009. Assembly and disassembly of the capsid-like external scaffold of immature virions during vaccinia virus morphogenesis. *J. Virol.* 83:9140–9150.
- Moss B, Rosenblum EN. 1973. Protein cleavage and poxvirus morphogenesis: tryptic peptide analysis of core precursors accumulated by blocking assembly with rifampicin. *J. Mol. Biol.* 81:267–269.
- Senkevich TG, White CL, Koonin EV, Moss B. 2002. Complete pathway for protein disulfide bond formation encoded by poxviruses. *Proc. Natl. Acad. Sci. U. S. A.* 99:6667–6672.
- Hiller G, Weber K. 1985. Golgi-derived membranes that contain an acylated viral polypeptide are used for vaccinia virus envelopment. *J. Virol.* 55:651–659.
- Toozé J, Hollinshead M, Reis B, Radsak K, Kern H. 1993. Progeny vaccinia and human cytomegalovirus particles utilize early endosomal cisternae for their envelopes. *Eur. J. Cell Biol.* 60:163–178.
- Schmelz M, Sodeik B, Ericsson M, Wolffe EJ, Shida H, Hiller G, Griffiths G. 1994. Assembly of vaccinia virus: the second wrapping cisterna is derived from the trans Golgi network. *J. Virol.* 68:130–147.
- Blasco R, Moss B. 1992. Role of cell-associated enveloped vaccinia virus in cell-to-cell spread. *J. Virol.* 66:4170–4179.
- Smith GL, Law M. 2004. The exit of vaccinia virus from infected cells. *Virus Res.* 106:189–197.
- Dales S, Mosbach EH. 1968. Vaccinia as a model for membrane biogenesis. *Virology* 35:564–583.
- Sodeik B, Krijnse-Locker J. 2002. Assembly of vaccinia virus revisited: de novo membrane synthesis or acquisition from the host? *Trends Microbiol.* 10:15–24.
- Husain M, Moss B. 2003. Evidence against an essential role of COPII-mediated cargo transport to the endoplasmic reticulum-Golgi intermediate compartment in the formation of the primary membrane of vaccinia virus. *J. Virol.* 77:11754–11766.
- Husain M, Weisberg AS, Moss B. 2006. Existence of an operative pathway from the endoplasmic reticulum to the immature poxvirus membrane. *Proc. Natl. Acad. Sci. U. S. A.* 103:19506–19511.
- Chlanya P, Carbajal MA, Cyrklaff M, Griffiths G, Krijnse-Locker J. 2009. Membrane rupture generates single open membrane sheets during vaccinia virus assembly. *Cell Host Microbe* 6:81–90.
- Maruri-Avidal L, Weisberg AS, Moss B. 2011. Vaccinia virus L2 protein associates with the endoplasmic reticulum near the growing edge of crescent precursors of immature virions and stabilizes a subset of viral membrane proteins. *J. Virol.* 85:12431–12441.
- Maruri-Avidal L, Weisberg AS, Bisht H, Moss B. 2013. Analysis of viral membranes formed in cells infected by a vaccinia virus L2-deletion mutant suggests their origin from the endoplasmic reticulum. *J. Virol.* 87: 1861–1871.
- Husain M, Weisberg AS, Moss B. 2007. Sequence-independent targeting of transmembrane proteins synthesized within vaccinia virus factories to nascent viral membranes. *J. Virol.* 81:2646–2655.
- Wolffe EJ, Moore DM, Peters PJ, Moss B. 1996. Vaccinia virus A17L open reading frame encodes an essential component of nascent viral membranes that is required to initiate morphogenesis. *J. Virol.* 70:2797–2808.
- Rodríguez JR, Risco C, Carrascosa JL, Esteban M, Rodríguez D. 1997. Characterization of early stages in vaccinia virus membrane biogenesis: implications of the 21-kilodalton protein and a newly identified 15-kilodalton envelope protein. *J. Virol.* 71:1821–1833.
- Unger B, Mercer J, Boyle KA, Traktman P. 2013. Biogenesis of the vaccinia virus membrane: genetic and ultrastructural analysis of the contributions of the A14 and A17 proteins. *J. Virol.* 87:1083–1097.
- Rodríguez JR, Risco C, Carrascosa JL, Esteban M, Rodríguez D. 1998. Vaccinia virus 15-kilodalton (A14L) protein is essential for assembly and attachment of viral crescents to virosomes. *J. Virol.* 72:1287–1296.
- Traktman P, Liu K, DeMasi J, Rollins R, Jesty S, Unger B. 2000. Elucidating the essential role of the A14 phosphoprotein in vaccinia virus morphogenesis: construction and characterization of a tetracycline-inducible recombinant. *J. Virol.* 74:3682–3695.
- Traktman P, Caligiuri A, Jesty SA, Sankar U. 1995. Temperature-sensitive mutants with lesions in the vaccinia virus F10 kinase undergo arrest at the earliest stage of morphogenesis. *J. Virol.* 69:6581–6587.
- Szajner P, Weisberg AS, Moss B. 2004. Evidence for an essential catalytic role of the F10 protein kinase in vaccinia virus morphogenesis. *J. Virol.* 78:257–265.
- Punjabi A, Traktman P. 2005. Cell biological and functional characterization of the vaccinia virus F10 kinase: implications for the mechanism of virion morphogenesis. *J. Virol.* 79:2171–2190.
- Resch W, Weisberg AS, Moss B. 2005. Vaccinia virus nonstructural protein encoded by the A11R gene is required for formation of the virion membrane. *J. Virol.* 79:6598–6609.
- Wu X, Meng X, Yan B, Rose L, Deng J, Xiang Y. 2012. Vaccinia virus virion membrane biogenesis protein A11 associates with viral membranes in a manner that requires the expression of another membrane biogenesis protein, A6. *J. Virol.* 86:11276–11286.
- Satheshkumar PS, Weisberg A, Moss B. 2009. Vaccinia virus H7 protein contributes to the formation of crescent membrane precursors of immature virions. *J. Virol.* 83:8439–8450.
- Maruri-Avidal L, Domínguez A, Weisberg AS, Moss B. 2011. Participation of

- vaccinia virus L2 protein in the formation of crescent membranes and immature virions. *J. Virol.* 85:2504–2511.
34. Meng XZ, Embry A, Sochia D, Xiang Y. 2007. Vaccinia virus A6L encodes a virion core protein required for formation of mature virion. *J. Virol.* 81:1433–1443.
 35. Moss B, Rosenblum EN, Katz E, Grimley PM. 1969. Rifampicin: a specific inhibitor of vaccinia virus assembly. *Nature* 224:1280–1284.
 36. Nagayama A, Pogo BGT, Dales S. 1970. Biogenesis of vaccinia: separation of early stages from maturation by means of rifampicin. *Virology* 40:1039–1051.
 37. Zhang Y, Moss B. 1992. Immature viral envelope formation is interrupted at the same stage by lac operator-mediated repression of the vaccinia virus D13L gene and by the drug rifampicin. *Virology* 187:643–653.
 38. Sodeik B, Griffiths G, Ericsson M, Moss B, Doms RW. 1994. Assembly of vaccinia virus: effects of rifampin on the intracellular distribution of viral protein p65. *J. Virol.* 68:1103–1114.
 39. Szajner P, Weisberg AS, Moss B. 2004. Physical and functional interactions between vaccinia virus F10 protein kinase and virion assembly proteins A30 and G7. *J. Virol.* 78:266–274.
 40. McCraith S, Holtzman T, Moss B, Fields S. 2000. Genome-wide analysis of vaccinia virus protein-protein interactions. *Proc. Natl. Acad. Sci. U. S. A.* 97:4879–4884.
 41. Yeh WW, Moss B, Wolffe EJ. 2000. The vaccinia virus A9L gene encodes a membrane protein required for an early step in virion morphogenesis. *J. Virol.* 74:9701–9711.
 42. Earl PL, Cooper N, Wyatt LS, Moss B, Carroll MW. 1998. Preparation of cell cultures and vaccinia virus stocks, p 16.16.1–16.16.3. In Ausubel FM, Brent R, Kingston RE, Moore DD, Seidman JG, Smith JA, Struhl K (ed), *Current protocols in molecular biology*, vol 2 John Wiley and Sons, New York, NY.
 43. Betakova T, Wolffe EJ, Moss B. 1999. Membrane topology of the vaccinia virus A17L envelope protein. *Virology* 261:347–356.
 44. Manders EM, Verbeek FJ, Aten JA. 1993. Measurement of co-localization of objects in dual-color confocal images. *J. Microsc.* 169:375–382.
 45. Graham JM. 2001. Isolation of Golgi membranes from tissues and cells by differential and density gradient centrifugation. *Curr. Protoc. Cell Biol.* Chapter 3:Unit 3.9. doi:[10.1002/0471143030.cb0309s10](https://doi.org/10.1002/0471143030.cb0309s10).
 46. da Fonseca FG, Weisberg A, Wolffe EJ, Moss B. 2000. Characterization of the vaccinia virus H3L envelope protein: topology and posttranslational membrane insertion via the C-terminal hydrophobic tail. *J. Virol.* 74:7508–7517.
 47. Senkevich TG, Wyatt LS, Weisberg AS, Koonin EV, Moss B. 2008. A conserved poxvirus NlpC/P60 superfamily protein contributes to vaccinia virus virulence in mice but not to replication in cell culture. *Virology* 374:506–514.
 48. Hegde RS, Keenan RJ. 2011. Tail-anchored membrane protein insertion into the endoplasmic reticulum. *Nat. Rev. Mol. Cell Biol.* 12:787–798.
 49. Grimley PM, Rosenblum EN, Mims SJ, Moss B. 1970. Interruption by rifampin of an early stage in vaccinia virus morphogenesis: accumulation of membranes which are precursors of virus envelopes. *J. Virol.* 6:519–533.
 50. Schuldiner M, Metz J, Schmid V, Denic V, Rakwalska M, Schmitt HD, Schwappach B, Weissman JS. 2008. The GET complex mediates insertion of tail-anchored proteins into the ER membrane. *Cell* 134:634–645.